small NANO MICRO

Silver Nanoparticles

# Silver Nanoparticle Exposure Attenuates the Viability of Rat Cerebellum Granule Cells through Apoptosis Coupled to Oxidative Stress

*Nuoya Yin, Qian Liu, Jiyan Liu, Bin He, Lin Cui, Zhuona Li, Zhaojun Yun, Guangbo Qu, Sijin Liu, Qunfang Zhou,* and Guibin Jiang*

*The impact of silver nanoparticles (AgNPs) on the central nervous system is a topic with mounting interest and concern and the facts remain elusive. In the current study, the neurotoxicity of commercial AgNPs to rat cerebellum granule cells (CGCs) and the corresponding molecular mechanism are closely investigated. It is demonstrated that AgNPs induce significant cellular toxicity to CGCs in a dose-dependent manner without damaging the cell membrane. Flow cytometry analysis with the Annexin V/propidium iodide (PI) staining indicates that the apoptotic proportion of CGCs upon treatment with AgNPs is greatly increased compared to the negative control. Moreover, the activity of caspase-3 is largely elevated in AgNP-treated cells compared to the negative control. AgNPs are demonstrated to induce oxidative stress, reflected by the massive generation of reactive oxygen species (ROS), the depletion of antioxidant glutathione (GSH), and the increase of intracellular calcium. Histological examination suggests that AgNPs provoke destruction of the cerebellum granular layer in rats with concomitant activation of caspase-3, in parallel to the neurotoxicity of AgNPs observed in vitro. Taken together, it is demonstrated for the first time that AgNPs substantially impair the survival of primary neuronal cells through apoptosis coupled to oxidative stress, depending on the caspase activation-mediated signaling.*

## 1. Introduction

Nanomaterials are becoming extremely popular in biological, medical, and biochemical engineering fields owing to their novel physical and chemical properties such as extraordinary electric, light-emitting, and catalytic properties, which differ from the conventional materials in many aspects.[1,2] Among the various nanotechnology products, silver nanoparticles (AgNPs) are emerging as one of the fastest-growing product categories and have the highest degree of commercialization.[3] They have been widely used in medical instruments, personal care products, food services, building materials, and textiles due to their excellent antibacterial effect.[4,5] AgNPs are marketed as deodorants, room sprays, laundry detergents, wall paints, and are also used for water purification and indoor air-quality management.[4,6,7] Thus, daily exposure of the consumers to AgNPs from many different sources could occur, which may increase the possibility of AgNPs entering human bodies, tissues, and cells.[8] Due to their small sizes, nanoparticles are more likely to travel through organs than larger particles, and may produce special biological effects on some organs. Preceding research revealed that silver nanoparticles could be accumulated in various organs including liver, kidney, testis, lung, and brain,[9] which provides the possibility of interfering with biological functions in organisms.

N. Yin, Dr. Q. Liu, Dr. J. Liu, Dr. B. He, Dr. L. Cui
Dr. Z. Li, Z. Yun, Dr. G. Qu, Prof. S. Liu, Dr. Q. Zhou
Prof. G. Jiang, State Key Laboratory of Environmental Chemistry and Ecotoxicology,
Research Center for Eco-Environmental Sciences
Chinese Academy of Sciences
PO Box 2871, Beijing 100085, China
E-mail: zhouqf@rcees.ac.cn
Tel/Fax: 86-10-62849179

DOI: 10.1002/smll.201202732

**Table 1** Characterization of AgNPs (n = 3)

| Dispersion medium | Particle size [nm] | | PDI | | Zeta potential [mV] | |
|---|---|---|---|---|---|---|
| | 0 h | 24 h | 0 h | 24 h | 0 h | 24 h |
| Culture medium | 22.8 ± 0.7 | 25.9 ± 0.3 | 0.12 ± 0.05 | 0.17 ± 0.06 | −13.5 ± 2.4 | −15.6 ± 1.7 |
| Aqueous solution | 21.7 ± 1.1 | 24.4 ± 0.6 | 0.11 ± 0.08 | 0.15 ± 0.04 | −5.8 ± 1.2 | −6.1 ± 0.9 |

Its toxicity evaluation is also very critical as AgNPs are used for biomedical, personal care, and other purposes related to human health.

Exposure to nanoparticles can occur via inhalation, dermal contact, and ingestion, thus leading to a wide variety of toxicological effects. Previous in vitro studies have shown that AgNPs have the potential to induce toxicity in cells derived from a variety of tissues, including skin, liver, lung, vascular system, and reproductive organs. Arora et al. found that AgNPs induced cell death and oxidative stress in human fibrosarcoma and skin carcinoma cells.[10] The subsequent studies from the same group revealed that AgNPs could enter cells, causing DNA damage and apoptosis in fibroblasts and liver cells.[11] A decrease of cell viability was observed in alveolar macrophages and lung epithelial cells treated with AgNPs.[12] AgNPs were also found to cause toxicity in germ line stem cells via a reduction in mitochondrial function, induction of lactate dehydrogenase (LDH) leakage, and apoptosis.[13] In vitro studies based on neural-like cell lines, such as PC12 cells (rat cell line with a neuronal-like phenotype) showed possible neural toxicity of AgNPs.[14]

It has been reported that AgNPs are translocated into blood circulation and accumulate in some organs, causing hepatotoxicity or renal toxicity when administered orally, inhaled, or admitted subcutaneously.[15,16] However, nanoparticles could not only cause adverse effects on primary organs which are directly exposed, but also in secondary locations such as the cardiovascular or central nervous systems (CNS), upon systemic circulation.[17] Particles on the nanoscale are capable of permeating the tight blood–brain barrier (BBB) by either carrier-mediated endocytosis or passive diffusion due to their small particle size.[18] It has been shown that AgNPs could come across through and be accumulated in an in vitro BBB model composed of primary rat brain microvessel vascular endothelial cells.[19] AgNPs were able to induce inflammation and affect the integrity of this BBB model, and then easily make their way to the brain.[20] Inhalation exposure studies suggested that inhaled nanoparticles may reach the brain through the nasopharyngeal system.[21] Ye and colleagues investigated the in vivo effects of AgNPs on hippocampal synaptic plasticity and spatial cognition in rats, and showed that AgNPs, through nasal administration, induced impairment of hippocampus function.[22] These results suggest the possibility of AgNPs causing neurotoxicity in humans and other animals, though the mechanism of its neurotoxicity is still to be studied.

Primary cell cultures isolated from target tissues, as a useful tool, are becoming popular in studies of toxicity, drug metabolism, and enzyme induction. They are desirable in cytotoxicity tests for medicines as this kind of model can simulate in vivo cell situations more closely.[23,24] Primary rat cerebellum granule cell cultures, having the characteristics of neural tissues, are thought a good model for neuron biological studies and are used here for in vitro studies on the toxicity of AgNPs and its potential mechanism. Herein, CGCs were exposed to different concentrations of AgNPs. Based on cell viability, cell morphology, and cellular membrane integrity, AgNP-induced cytotoxicity was determined. The apoptosis of CGCs caused by AgNPs was determined through the Annexin V/propidium iodide (PI) staining assay using flow cytometry and the evaluation of the intracellular activated caspase-3 enzyme. Oxidative stress, as the best-known factor for apoptosis, was assessed by measuring the reactive oxygen species (ROS) levels, glutathione (GSH) levels, and calcium influx in CGCs. Finally, neonatal SD rats, as an in vivo model, were used to evaluate AgNP-induced neurotoxicity by histopathological analysis.

## 2. Results

### 2.1. AgNP Characterization

The AgNP solution used in this study was characterized by TEM and dynamic light scattering (DLS) and the physicochemical properties of the AgNPs are summarized in **Table 1**. The morphology of AgNPs observed by TEM (**Figure 1**A) showed that they were uniformly spherical in shape, with a narrow size distribution. The DLS measurement was executed in both the cell culture medium and aqueous solution at two time points (0 h, 24 h). The results (Figure 1B) showed that the average size of AgNPs exhibited a slight shift from 22.8 ± 0.7 nm to 25.9 ± 0.3 nm in culture medium and from 21.7 ± 1.1 nm to 24.4 ± 0.6 nm in aqueous solution, with polydispersity index (PDI) less than 0.25, indicating that the AgNPs were stable over 24 h without agglomeration in both the culture medium and aqueous solution. The zeta potential for AgNPs was -13.5 ± 2.4 mV in culture medium and -5.8 ± 1.2 mV in aqueous solution. The negative zeta potential of the Ag particles ensured that the AgNP solution had high stabil-ity and could resist aggregation to some extent. Moreover, during our experimental period (three months), no obvious aggregation was found in the stock solution and it stayed homogeneous, ensuring the consistency of the experiments with different incubation times.

NANO MICRO small

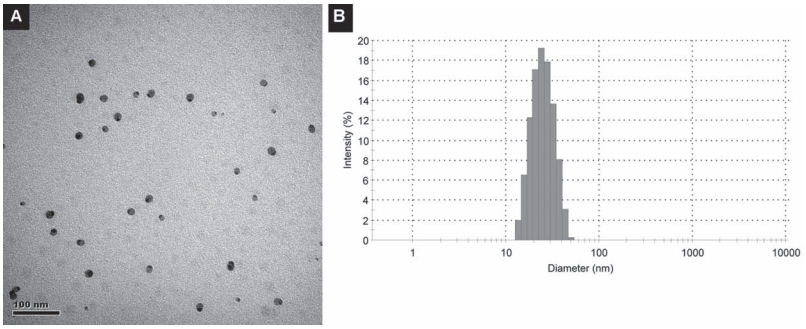


**Figure 1.** Characterization of AgNPs. (A) Transmission electron microscopy (TEM) image of AgNPs. (B) The particle size distribution of AgNPs dispersed in the culture medium with serum by dynamic light scattering.

### 2.2. AgNPs Cause Cytotoxicity in CGCs

Cell viability of CGCs was evaluated after AgNPs exposure for 24 h based on an AB staining assay. The results shown in **Figure 2**A indicate that cell viability declined with the increase in exposure levels of AgNPs, and the calculated $IC_{50}$ of AgNPs is 0.96 ± 0.12 μg/mL. Compared with other cell lines reported in previous papers,[25,26] the $IC_{50}$ of AgNPs for CGCs is the lowest, showing that CGCs are a much more sensitive cell model for AgNP exposure.

Morphological observation (Figure 2B) of AgNP-exposed CGCs using confocal microscopy after the staining by Live-Dead cell staining kit showed that the control group treated with cell culture medium alone has normal soma and synapses. More than 90% of CGCs have green fluorescence, showing the high cell viability. However, the CGCs treated with 1 μg/mL AgNPs for 24 h have obvious cell-body shrinkage, as the neuronal synapses are fewer and shorter than the controls. The living cells (green fluorescence) dramatically decreased, and the dead cells (red fluorescence) increased in number, indicating that AgNPs can greatly reduce the cell viability of CGCs.

In order to investigate the cell membrane integrity after AgNP exposure, we measured extracellular lactate dehydrogenase (LDH) levels. As shown in Figure 2C, measurement of CGCs exposed to 0.01-2.5 μg/mL of AgNPs for 24 h showed little fluctuations in extracellular LDH levels compared with the negative control, suggesting AgNP exposure did not damage the cell membrane, and the leakage of intracellular LDH did not therefore occur. However, the same range (0.05–2.5 μg/mL) of AgNPs obviously decreased the viabilities of CGCs, implying that the AgNP-induced cell death is dominantly triggered by apoptosis instead of necrosis, which may cause the obvious loss of cellular membrane integrity.

### 2.3. Cellular Apoptosis is Induced by AgNPs in CGCs

Based on the flow cytometry approach, the percentage of living cell (Q3 phase), early apoptotic (Q4 phase), late apoptotic (Q2 phase), and necrotic cell (Q1 phase) areas

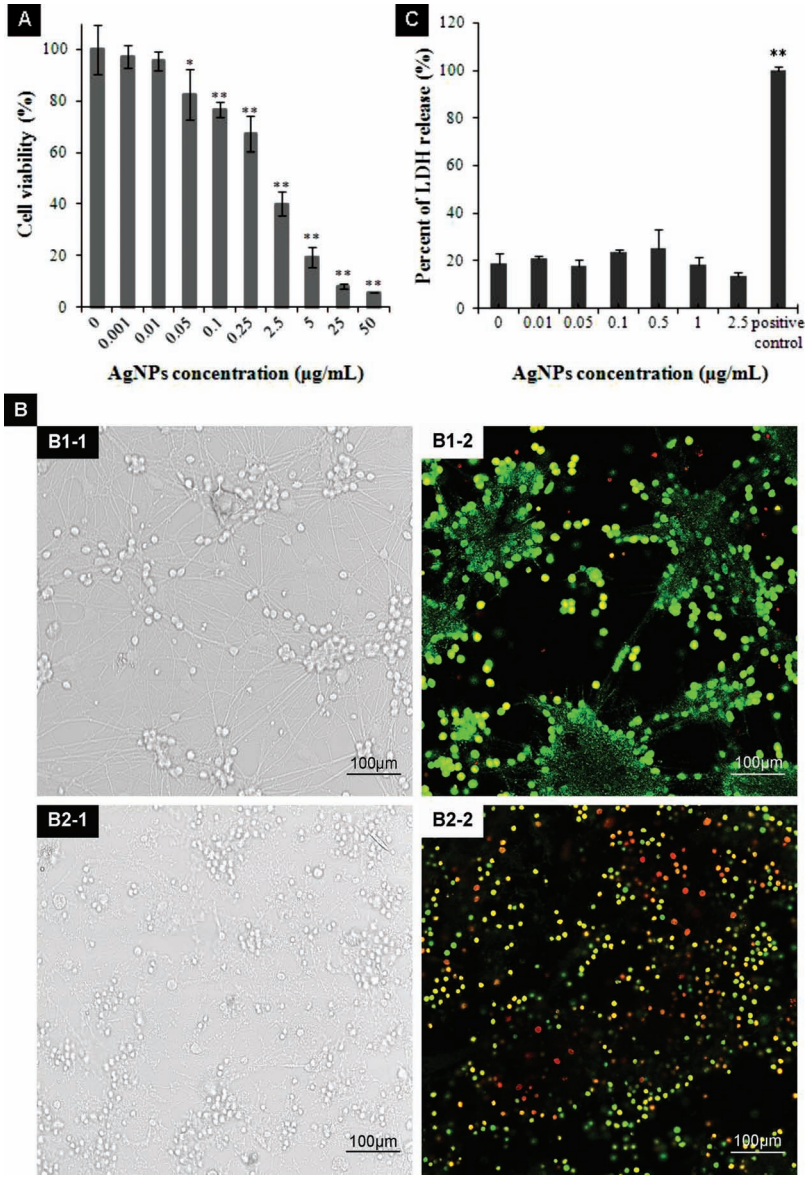


**Figure 2.** AgNP exposure induces cytotoxicity in CGCs. (A) Dose-response curve for AgNPs inducing cell death in CGCs (24 h). (B) Morphological characterization of CGCs with or without AgNP treatment using Live-Dead Cell Staining Kit. B1-1: negative control, bright field image; B1-2: negative control, fluorescence image; B2-1: AgNPs (1 μg/mL, 24 h), bright field image; B2-2: AgNPs (1 μg/mL, 24 h), fluorescence image. (C) Extracellular LDH evaluation for AgNP-exposed CGCs (24 h). $H_2O_2$ (1 mM) was used as the positive control. The results were presented as mean ± SD. $*P < 0.05$ and $**P < 0.005$, versus negative control.

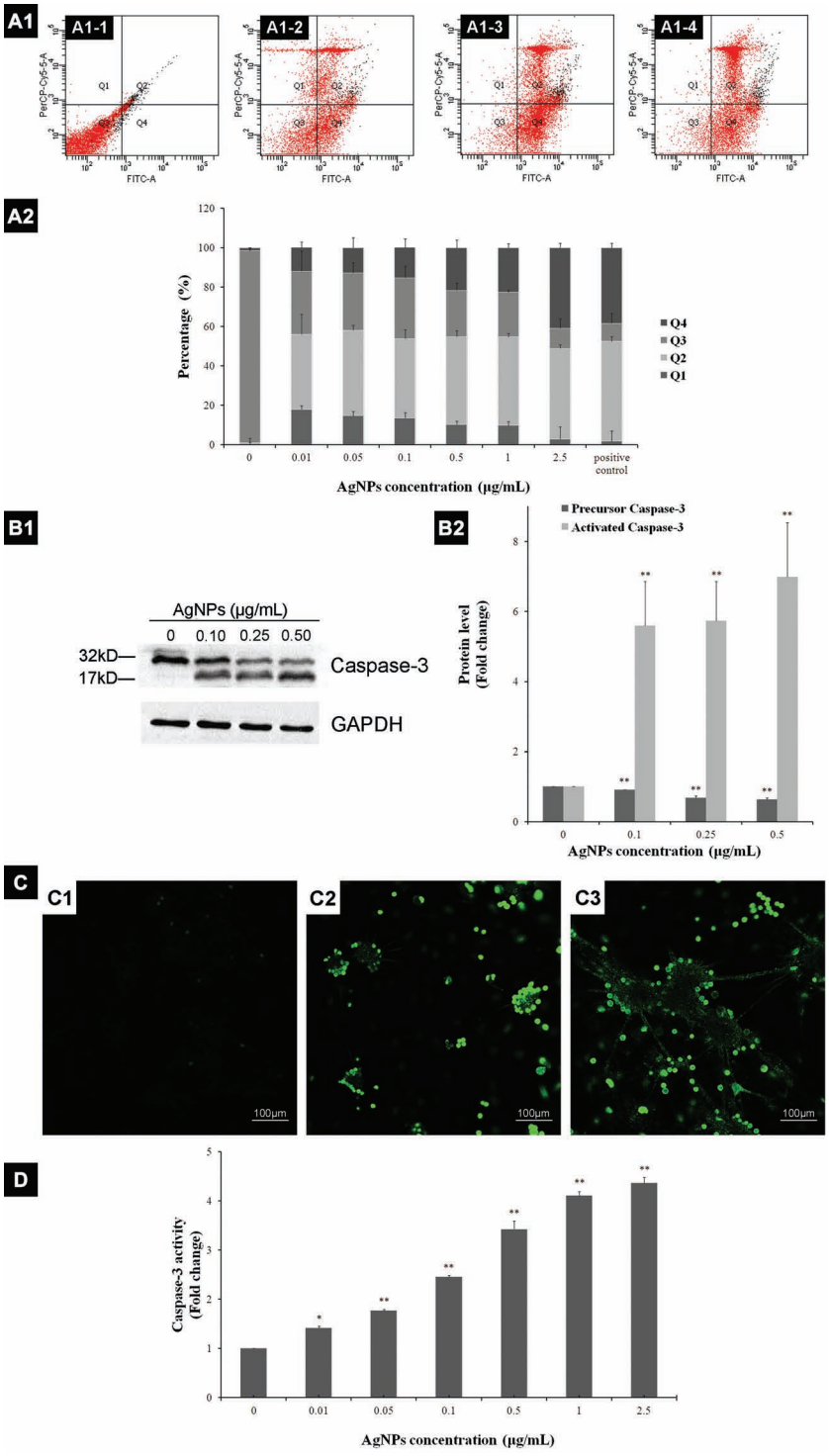


**Figure 3.** AgNP exposure induces apoptosis in CGCs. (A) Apoptotic rate of CGCs treated with AgNPs based on flow cytometric analysis. (A1) The phase distribution of cells stained with the Annexin V-FITC and PI. Notes: (A1-1) Negative control, (A1-2) 0.05 μg/mL AgNPs, (A1-3) 2.5 μg/mL AgNPs, (A1-4) 1 mM $H_2O_2$ (positive control). (A2) Dose-response of AgNPs for apoptotic rate in CGCs. (B) Western blot analysis of caspase-3 expression in AgNP-treated CGCs (37 °C, 24 h). (B1) Precursor and activated caspase-3 proteins were detected using specific antibodies. (B2) The levels of precursor and activated caspase-3 were quantified based on grey levels of the band in **Figure 3**B1. The levels of the negative control were normalized as 1. (C) The immunofluorescence staining of activated caspase-3 in CGCs with medium (C1), AgNPs (1 μg/mL, C2) and $H_2O_2$ (1 mM, C3) treatment. (D) The intracellular protein levels of activated caspase-3 in AgNP-treated CGCs (24 h) based on Caspase-Glo Assay. The data are presented as mean ± SD. $*P < 0.05$ and $**P < 0.005$, versus negative control.

were evaluated for the AgNP-exposed CGCs. As shown in **Figure 3**, AgNPs could induce obvious apoptosis in CGCs (Figure 3A1) and the apoptotic proportion was raised with the increase in exposure dose (Figure 3A2). For example, the early apoptotic percentage (Q4) increased from 13.8 ± 3.1%, to 21.0 ± 4.7% and to 44.1 ± 6.9%, and the late apoptotic percentage (Q2) increased from 30.1 ± 10.4% to 44.5 ± 3.7% and to 50.3 ± 5.0%, after treatment with AgNPs at concentrations of 0.01 μg/mL, 0.5 μg/mL, and 2.5 μg/mL, respectively. These results confirm that AgNPs can induce CGC death in a concentration-dependent manner, mainly mediated through apoptotic mechanisms.

To further evidence that AgNPs induce cellular apoptosis, we used caspase-3 as a biomarker. Western blot analysis of AgNP-treated CGCs (Figure 3B1) showed that in the negative control group only precursor caspase-3 (32 kD) was detected, while in AgNP-treated cells (0.1, 0.25, 0.5 μg/mL, 37 °C, 24 h), both the intact caspase-3 and 17 kD cleaved product (activated caspase-3) were detected. Further, the levels of precursor and activated caspase-3 were quantified based on grey levels of the band in Figure 3B1. It was interesting to find that the precursor of caspase-3 reduced with the increase in AgNP exposure levels, while the activated form went the opposite way (Figure 3B2). The up-regulated activated form of caspase-3 was indicative of apoptosis induced by AgNPs. Immunofluorescence observations of activated caspase-3 by confocal microscopy staining with cleaved caspase-3 antibody showed that the negative control group had no green fluorescence, implying the apoptotic level was extremely low in the normal CGCs (Figure 3C1), while the positive control with $H_2O_2$ (1 mM) revealed strong green fluorescence, which indicates more activation of caspase-3 (Figure 3C3). In the AgNP treatment group (1 μg/mL, 24 h), obvious green fluorescence could be observed (Figure 3C2), showing the existence of activated caspase-3, which was consistent with the western blot results. Quantification of activated caspase-3 in CGCs showed that AgNPs (0.01-2.5 μg/mL) could significantly increase activated caspase-3 levels, which were around 1.5-4 fold higher than for the negative control, confirming the higher expression of activated caspase-3 in CGCs under AgNP

NANO MICRO small

exposure. Thus, AgNP-induced CGC apoptosis is mediated through a caspase-dependent signaling pathway involved with caspase-3.

### 2.4. AgNPs Can Cause Oxidative Stress in CGCs

It has been widely reported that reactive oxygen species (ROS) generation and oxidative stress lead to apoptotic cell death.[27] Based on the measurement of ROS and GSH levels, the possibility of oxidative stress caused by AgNP exposure was assessed in CGCs. The results of ROS formation detected by DCFH-DA assay[28] showed that the fluorescent intensity in the negative control was 9.77 ± 0.70 F.U., while it was 27.15 ± 3.83 F.U. for the positive control (1 mM $H_2O_2$). As for AgNP exposure groups, the fluorescent intensity was significantly enhanced when the AgNP concentration was higher than 0.25 μg/mL (**Figure 4**A), showing the accumulation of intracellular ROS under AgNP exposure, which is consistent with previous findings for HepG 2 cells.[26]

Glutathione (GSH), as an antioxidant, can prevent cellular damage caused by reactive oxygen species.[29] GSH depletion is one of the crucial events in the apoptotic process, induced by various apoptotic signals.[30] To investigate the intracellular GSH levels of CGCs, the cells were loaded with various concentrations of AgNPs for 4 h. Figure 4B showed that GSH levels were significantly exhausted in AgNP-exposed CGCs as compared with the negative control ($P < 0.05$), and the depletion of GSH followed a dose-dependent manner. The increase of ROS and the decrease of GSH levels in CGCs with AgNP treatment indicated that AgNPs could cause oxidative stress in CGCs by disturbing the cellular antioxidant defense system.

Calcium ions ($Ca^{2+}$) play a crucial role in cellular processes. $Ca^{2+}$-dependent depolarization of mitochondria has been suggested to contribute to oxidative stress in neuronal injury through the production of ROS.[31] The influence of AgNPs on intracellular calcium influx was evaluated by measuring the changes of intracellular-free calcium ions in AgNP-treated CGCs using the membrane permeable $Ca^{2+}$-binding fluorescent probe Fura-2/AM. The results shown in Figure 4C demonstrated that AgNP exposure immediately promoted calcium ions in CGCs and reached the maximal fluorescence intensity after 5-6 min. This effect was also concentration-dependent. The maximum response in the group treated with 2.5 μg/mL of AgNPs was about twofold that of the negative control. These results further confirm that AgNPs could provoke an increase in intracellular calcium ions and perturbations in intracellular calcium levels, thus causing oxidative stress in CGCs.

### 2.5. AgNPs May Cause In vivo Neurotoxicity in Natal rats

To investigate the penetration of AgNPs in rat cerebellum, the total silver content of cerebellum tissue was measured by ICP-MS and the results are shown in **Figure 5**A. A dose-related elevation of silver levels were observed in cerebellum,

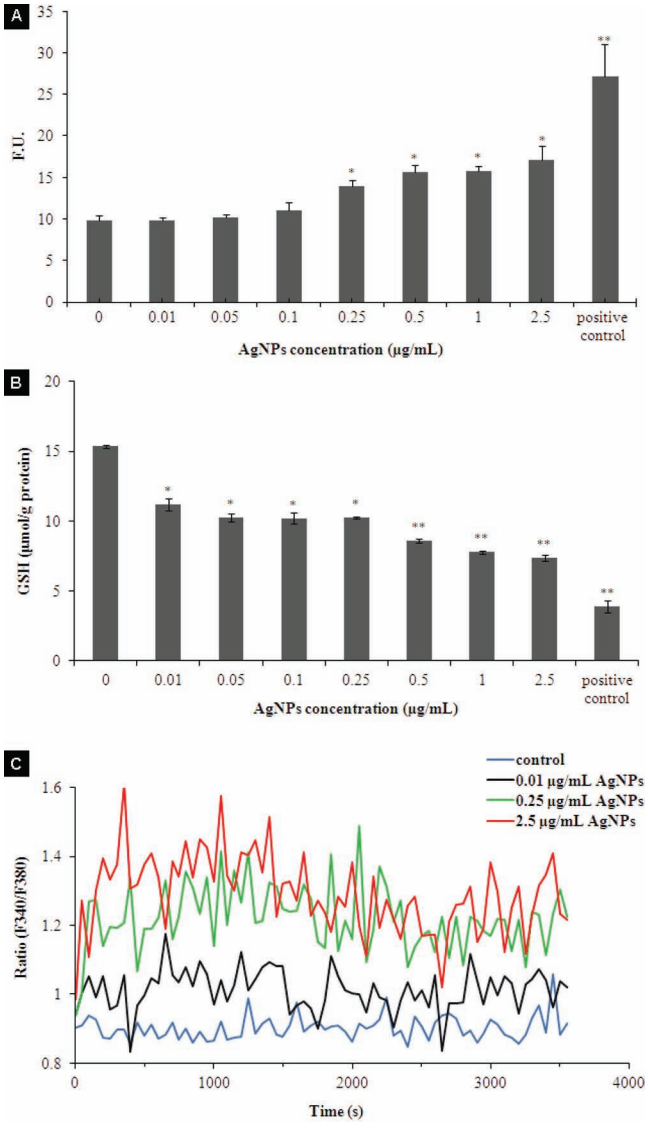


**Figure 4.** AgNP exposure causes oxidative stress in CGCs. (A) ROS levels in CGCs treated with AgNPs or $H_2O_2$ (1 mM). (B) Intracellular GSH in CGCs treated with AgNPs or $H_2O_2$ (1 mM). (C) Changes of intracellular calcium ions in AgNP-treated CGCs. The results were presented as mean ± SD. $*P < 0.05$ and $**P < 0.005$, versus negative control.

showing that AgNPs might be capable of penetrating the BBB, thus accumulating in the cerebellum tissue when administered through intranasal instillation.

The body weight was monitored weekly for both controls and AgNPs exposed rats during the whole experiment to evaluate the possible general toxicity of AgNPs. The average of weight gain rates were 15.1 ± 4.8 g/week, 15.2 ± 4.9 g/week, 14.9 ± 5.1 g/week, 14.6 ± 5.2 g/week, and 14.3 ± 5.3 g/week for the control, the 0.05, 0.1, 0.2, and 1 mg/kg AgNP exposure groups, respectively, showing no significant difference among these groups. Daily observation of the physiological status of the AgNP-exposed rats indicated no obvious abnormal behavior for the AgNP-exposed rats for 21 consecutive days. It was thus thought that no general toxicity was caused by AgNPs at current tested levels during the 21 day period.

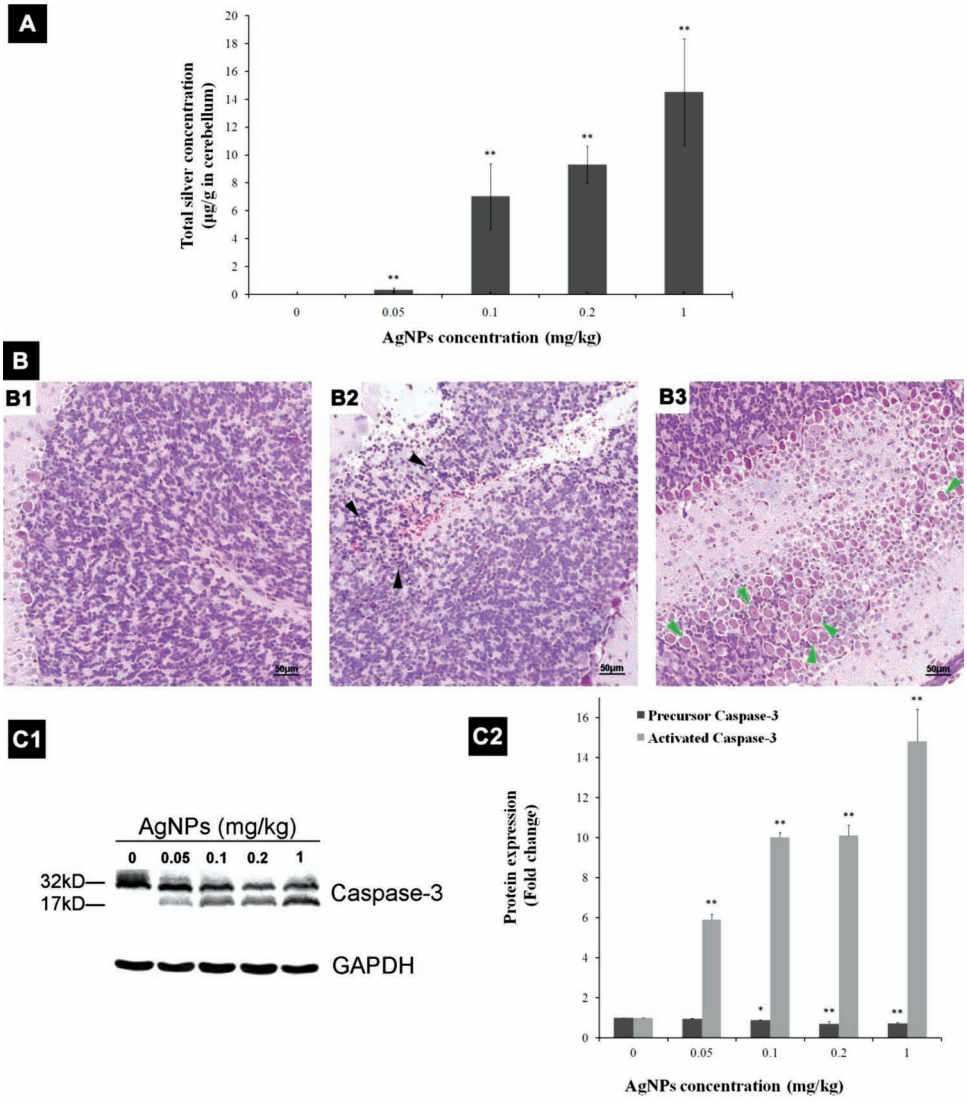


**Figure 5.** AgNP exposure induces neurotoxicity in natal rat cerebellum. (A) The total silver content of cerebellum tissue measured by ICP-MS. All the groups were administered with AgNP nasal drops or the vehicle control once a day for 21 consecutive days. (B) Histopathological observations in cerebellum sections by H&E staining. (B1) Cerebellum section of control. (B2) Cerebellum section of rat treated with 0.2 mg/kg AgNPs. Granule cells had abnormal shape with smaller sizes and shrinking nucleus (black arrow). (B3) Cerebellum section of rat treated with 1 mg/kg AgNPs. A huge amount of CGCs lost in the granular layer, with more Golgi cells appeared apparently (green arrow). (C) Caspase-3 expression in rat cerebellum treated with AgNPs for 21 consecutive days. (C1) Precursor and activated caspase-3 were detected using specific antibodies. (C2) The levels of precursor and activated caspase-3 were quantified based on grey levels of the band in Figure 5C1. The levels of the negative control were normalized as 1. The results were presented as mean ± SD. $*P < 0.05$ and $**P < 0.005$, versus negative control.

To survey the neuronal injury induced by AgNPs, Hematoxylin-eosin (H&E) staining of cerebellum sections was performed and the results are shown in Figure 5B. The normal morphology of granular layer containing a dense cluster of granule cells and some Golgi cells was observed in control rats (Figure 5B1). Obvious alterations in the morphology of granular layer appeared in AgNP-exposure groups. For example, in the cerebellum section of the rat treated with 0.2 mg/kg of AgNPs, a multitude of granule cells had an abnormal shape with a smaller size and shrinking nucleus, and a degenerated granular layer with loose and separated structure appeared in the cerebellum section as demonstrated in Figure 5B2. In the cerebellum section of the rat treated with 1 mg/kg of AgNPs, a huge amount of CGCs were lost in the granular layer, with a clear edema phenomenon as well as some necrotic areas (Figure 5B3). The histological findings in rat cerebellum reveal that AgNPs may produce significant neurotoxicity, which is possibly related to the exposure dose of AgNPs applied.

Possible apoptosis induced by AgNPs in natal rat cerebellum was also evaluated by the analysis of caspase-3 using western blot. The results shown in Figure 5C illustrate that caspase-3 was activated in rats treated with various concentrations of AgNPs (ranging from 0.05 to 1 mg/kg) for 21 consecutive days. Similar to the results obtained from CGCs, the

small NANO MICRO

precursor caspase-3 (32 kD) was down-regulated, following an increase in exposure dose, while the activated caspase-3 (17 kD) showed the opposite trend. These findings reveal that AgNP-induced neurotoxicity in rat cerebellum involves the activation of caspase-3, possibly associated with apoptosis.

## 3. Discussion

Up to now, a large number of studies indicate that AgNPs are toxic to cells derived from a variety of organs, and in vivo studies have demonstrated that AgNPs administered by inhalation, ingestion, or intra-peritoneal injection are capable of causing toxicity in several organs.[22,32–35] Moreover, nanoparticles can enter the brain by disruption of the blood–brain barrier (BBB) or be taken up directly into the brain by trans-synaptic transport.[18,21] The issue of assessing the specific responses of neurons to AgNPs is therefore of great relevance, given the crucial roles which they play. However, information on the effect of AgNPs on neuronal cells is very scarce. In our study, evidence that AgNPs can affect neuronal proliferation by stimulating apoptotic processes, with the mechanism of oxidative stress, is provided. This is consistent with earlier work in fibroblast, muscle, and colon cells.[10,36]

Time courses for the cytotoxicities of AgNPs were firstly screened based on different endpoints such as cell viability, LDH assay, and apoptosis. The results from some assays like extracellular LDH indicated that it was a not a very critical factor for the evaluation of the biological effect of AgNPs (data not shown). Twenty four hours, as the previous commonly selected time point,[10,26,37,38] was used for all in vitro experiments to ensure the possible comparison of the results herein with the others. Based on the cytotoxicity studies of nanoparticles in different kinds of cell lines,[27,39,40] AgNP were reported to induce significant cellular toxicities in different models. For example, the viability of liver cells and skin cells treated with AgNPs at 10 μg/mL for 24 h was reduced to about 70% and 58%, respectively.[41,42] By contrast, the viability of CGCs treated with AgNPs at the same concentration (10 μg/mL) for the same period of time (24 h) was reduced to about 11%, suggesting that AgNPs caused higher toxicity to CGCs. Compared with other cell lines,[25,26] the $IC_{50}$ of AgNPs for CGCs is the lowest, showing that CGCs are a much more sensitive cell model for AgNP evaluation.

Indeed, nanoparticles are mobile solids, which combine the properties of solids with the ability to move (a property of molecules).[43] There is a general agreement that dissolved Ag ions are responsible for the biocidal activity of AgNPs. Based on our previous report, free $Ag^+$ in CGCs culture medium was less than 1%.[26] The physicochemical properties of AgNPs measured by DLS showed that AgNPs were stable in the culture medium during the exposure period (24 h). Comparison of the inhibitory effects of AgNPs and silver nitrate on CGCs also demonstrated that AgNPs are more effective in cell growth inhibition than ionic silver ($IC_{50}$ of AgNPs and silver ions were 0.96 ± 0.12 μg/mL and 4.01 ± 0.63 μg/mL, respectively). Similar results were reported for other NPs. For example, Brunner et al. showed that iron oxide nanoparticles exhibited higher toxicity by a nanoparticle-specific cytotoxic mechanism than the dissolved ions.[44] It could thus be speculated that AgNPs themselves contribute to the cellular toxicities instead of the free $Ag^+$. Furthermore, the presence of AgNPs in neuronal cells confirmed by TEM–energy dispersive X-ray spectrometry after subcutaneous exposure directly offered the possibility that AgNPs exert influence over biological functions in the brain.[45]

Cell death caused by AgNPs from the AB assay was confirmed by the result from the Live-Dead Cell Staining Kit, in which assay, the obvious red fluorescence from cells stained with PI (which could indicate both necrotic and late apoptotic cells) was observed. The LDH assay revealed that AgNPs (0.01-2.5 μg/mL) had little effect on the cell membrane integrity, implying CGC death could be possibly associated with apoptosis. The Annexin V/PI staining assay is very useful in providing information on the mechanism of cell death (i.e., apoptosis or necrosis).[46] As shown in Figure 3A, the decrease of neuronal proliferation induced by AgNPs could be correlated with the activation of a mechanism of apoptotic death, as revealed by an increase in the rates of Annexin V-$FITC^+$/$PI^-$ (Q4 phase) and Annexin V-$FITC^+$/$PI^+$ (Q2 phase) based on flow cytometry. As for the mechanism of AgNP-induced cell death, this could be controversial. To further explain how the high staining rate of PI in AgNP-treated cells from the Live-Dead Cell Staining Kit was caused by late apoptosis instead of necrosis, we may speculate changes to the cell membrane permeability under certain situations, like chemical exposure.[47] We know that the molecular weights of PI and LDH were 668 Da and 135-140 kDa, respectively. It could be possible for the small molecular PI to penetrate into cell membranes to stain the neuron when the permeability was increased by AgNP exposure, while LDH a with relatively high molecular weight was still prevented from leaking out of the cells because the cells maintained membrane integrity. That could be the reason that AgNP-treated cells showed increased PI staining while the extracellular LDH level was kept at the basal level, showing AgNP-induced cell death was triggered by cell apoptosis. A similar phenomenon was reported in other primary cultured cells.[48] The cerebellar granule neurons which were morphologically clearly disintegrated and positively stained with trypan blue and propidium iodide only released about 45-50% of the intracellular LDH.[49]

Although diverse mechanisms including apoptosis, autophagy and necrosis were widely discussed in neuronal cell death,[50,51] the family of cysteine proteases—termed caspases—was a hot topic in this field.[50] It has been reported that the activation of caspases is responsible for regulating the apoptosis program and caspase-3 activation is often regarded as the point of no return in apoptosis.[52,53] To support our hypothesis of apoptosis induction by AgNPs, we further examined the activity of caspase-3 enzyme. Analysis by western blot (Figure 3B), immunofluorescence observation (Figure 3C), and quantification of activated caspase-3 enzyme (Figure 3D) all confirmed that caspase-3 was involved in AgNP-mediated CGC apoptosis. Caspase-dependent apoptosis has been previously shown to occur in response to treatment with other nanomaterials, such as nickel ferrite nanoparticles,[54] titanium dioxide

  

nanoparticles,[55] and metallic nickel nanoparticles.[56] Preceding works have demonstrated that other regulators were also involved in AgNP-induced apoptosis in other cell lines, for instance, involvement of the mitochondria-dependent JNK pathway in NIH3T3 fibroblast cells,[36] and DNA damage through disruption of the mitochondrial respiratory chain in human lung fibroblast cells (IMR-90) and human glioblastoma cells (U251).[57]

Various factors including ROS, decreased growth-factors, and genetic mutation can contribute to initiate the caspase-3 mediated apoptosis pathway.[58] Investigation on the other key player in AgNP-induced CGCs apoptosis herein showed that AgNPs could induce oxidative cell damage in CGCs through evoking ROS, which was further validated by depletion in GSH levels (Figure 4), as previous reports showed that nanomaterials could provoke oxidative stress, a common mechanism of cell damage.[59–61] Besides, $Ca^{2+}$-dependent depolarization of mitochondria has been suggested to contribute to oxidative stress in neuronal injury through the production of ROS.[31] As data presented here, AgNPs could also provoke an increase in intracellular calcium. There is also evidence that several kinds of nanomaterials could disturb the intracelluar calcium homeostasis, such as ZnO,[62] $TiO_2$,[63] Au,[64] and silica.[65] Anyhow, the generation of ROS, depletion of GSH and elevation of intracellular calcium indicated that oxidative stress should be the primary mechanism for AgNP-induced apoptosis in CGCs. Other reports have demonstrated a similar deleterious mechanism of AgNPs in fibroblast, muscle and colon cell lines.[10,36]

There is little doubt that programmed cell death (i.e. apoptosis) plays a major role in many neurodegenerative diseases, including Alzheimer's, Parkinson's and Huntington's diseases, stroke, and amyotrophic lateral sclerosis.[66,67] Besides, it has been shown that AgNPs were capable of pentrating through the BBB and accumulating in different brain regions.[15] Thus, AgNPs might induce the neuronal degeneration in the exposed animals by producing apoptosis. On the basis of our research in vitro, neonatal SD rats were administered with AgNPs by intranasal instillation, which is in line with previous report.[22] ICP-MS analysis demonstrated the dose-related existence of silver in the brain tissue, which could offer the possibility of the biological effect exerted by AgNP administration. This was in correspondence with previous studies as well.[68–70] Histological studies revealed that AgNPs in vivo caused the destruction of cerebellum granular layer, which was also involved with the activation of caspase-3, confirming the neurotoxicity of AgNPs in rat cerebellum. Although there are some other studies indicating the neurotoxicity could be observed in the brain after systemic, intracerebral, and intranasal administration of AgNPs.[22,71], it is still a hot topic for the speciation of AgNPs in vivo. It was ever reported that aluminum and copper nanoparticles were capable of inducing the same effects due to the presence of metal-containing nanoparticles,[72,73] and AgNPs was ever found in neuronal cells after subcutaneous exposure.[45] Despite this available information, more evidence is still needed to clarify the speciation of AgNPs in vivo and their biological effects.

## 4. Conclusion

In summary, we have shown that silver nanoparticles (AgNPs) produce significant cytotoxicity to rat cerebellum granule cells (CGCs), but have little effect on the cell membrane integrity. The Annexin V/PI assay via flow cytometry demonstrated that AgNPs induce CGC death through apoptosis. Quantitative analysis of the intracellularly activated caspase-3 enzyme demonstrates that caspase-3 is involved in AgNP-mediated CGC apoptosis in vitro, which is validated by western blot and immunofluorescent analysis. Moreover, oxidative stress is the expected mechanism for apoptosis as AgNPs could induce oxidative cell damage by inducing ROS generation, depleting GSH levels and disturbing the calcium homeostasis. In vivo studies showed the dose-related occurrence of Ag in the rat cerebellum tissue through intranasal instillation. AgNP exposure exerted significant neurotoxicity to rat cerebellum by destruction of the cerebellum granular layer, which was also involved with the activation of caspase-3. Overall, the data suggest AgNP-induced neuronal cell death through apoptosis, mediated by a caspase-dependent signaling pathway, with the mechanism of oxidative stress.

## 5. Experimental Section

### 5.1. AgNP Characterization

AgNP solution ($1 \times 10^4$ μg/mL) was purchased from HuZheng Nanotechnology Limited Company (Shanghai, China). Following to the instructions, the AgNPs were protected with 0.2% PVP. The morphology of AgNPs was characterized by transmission electron microscopy (TEM, Hitachi H-7500, Japan). The particle size distribution and zeta-potential of the AgNPs were measured by Malvern Zetasizer Nano ZS (Malvern, UK) at 25 °C.

The AgNP stock solution was prepared by resuspending the silver nanoparticles with deionized water, where silver nanoparticles were removed from the supernatant by centrifuging. The stock solution was maintained at 4 °C. A series of working solutions were freshly made by diluting the stock solution with distilled water or cell culture medium before use.

### 5.2. Cell Cultures

Primary cultured neurons were isolated mainly as described previously.[74] The primary cultured cerebellum granule cells (CGCs) were prepared from 7-day-old SD rat pups. The cerebellum of SD rat was dissociated in high-glucose HBSS (GIBCO, USA) and plated at $5 \times 10^5$ cells/mL in 96-well plates or $1 \times 10^6$ cells/mL in 6-well plates (Corning, USA), and all the plates were coated with poly-L-lysine (0.01%, Sigma-Aldrich, USA) beforehand. CGCs were cultured in DMEM-F12 (Hyclone, USA) supplemented with horse serum (5%, GIBCO, USA), fetal bovine serum (5%, GIBCO, USA), KCl (25 mM, Sigma-Aldrich, USA), L-glutamine (1%, Hyclone, USA) and antibiotics (penicillin 100 U/mL and streptomycin

NANO MICRO small

100 μg/mL, GIBCO, USA) at 37 °C in 5% $CO_2$ atmosphere. Arabinofuranosylcytosine (10 μM, Fluca, USA) was added to the culture medium after plating for 18-22 h to prevent proliferation of non-neuronal cells. The cells were cultured for 7 days until synapses formed.

### 5.3. Cellular Toxicity Evaluation

*Cell Viability Using AB Assay*: To measure the cytotoxicity of AgNPs to CGCs, various concentrations of AgNPs (0-50 μg/mL) were added. After exposure for 24 h, the cell viability was determined using AB assay as described previously.[75] The fluorescence was measured using excitation wavelength of 530 nm and emission wavelength of 590 nm in a multiwell fluometric reader (Thermo, USA).

*Cell Morphology Evaluation*: CGCs were exposed to AgNPs (1 μg/mL) for 24 h, then stained with Live-Dead Cell Staining Kit (Biovision, USA) following the protocol in the specifications. Finally the cells were photographed by a laser scanning confocal microscope (Leica, TSC SP5, USA).

*Cellular Membrane Integrity*: The cells were exposed to various concentrations of AgNPs (0-2.5 μg/mL); $H_2O_2$ (1 mM) was used as the positive control. After exposure for 24 h, the cell medium was collected and LDH activity was determined according to the manufacturer's instruc-tions (Promega, LDH Assay kit, USA).

### 5.4. Cell Apoptosis Analysis

*Evaluation of Cell Apoptosis Rate by Flow Cytometry*: To quantify the apoptotic cells, the staining of apoptotic cells was performed using the Annexin V-FITC/PI Apoptosis Detection Kit (BD Pharmingen, Heidelberg, Germany) according to the manufacturer's instruction. CGCs treated with different concentrations of AgNPs for 24 h were collected and resuspended in binding buffer. The cells were analyzed by flow cytometry (FACSVerse, BD, USA). About 10 000 events were acquired for flow-cytometric analysis.

*Intracellular Caspase-3 Expression by Western Blot*: CGCs were treated with different concentrations of AgNPs for 24 h. Collected cells were lysed on ice for 30 min in RIPA lysis buffer containing a mixture of protease inhibitors (Roche, EDTA-free Protease Inhibitor Cocktail Tablets, USA). Equal amounts of total proteins extracted from CGCs of different groups were loaded onto a 10% SDS-PAGE for separation and transferred onto the nitrocellulose membrane (PALL, USA). For immunoblotting, the nitrocellulose membrane was incubated with TBS-T containing non-fat milk (5%) for 1 h and then blotted with caspase-3 primary antibody (Cell Signaling Technology, USA) against specific proteins overnight at 4 °C. After washing with TBS-T, the membrane was further incubated with horseradish peroxidase (HRP)-labeled secondary antibody (goat anti rabbit IgG, Santa Cruz, USA) for 1 h at room temperature. Finally, the membrane was incubated with the signal substrate (PIERCE, USA) and exposed to X-rays (film from Kodak, China) for development.

*Immunofluorescent Analysis of Activated Caspase-3*: To analyze activated caspase-3, CGCs were immuno-stained with cleaved Caspase-3 Antibody (Alexa Fluor 488 conjugate, Cell Signaling Technology, USA) after exposure to AgNPs (1 μg/mL) or $H_2O_2$ (1 mM, as the positive control) for 24 h. Then cells were examined by a confocal microscope.

*Analysis of Intracellular Caspase-3 Enzyme Levels*: The measurement of the intracellular protein levels of activated caspase-3 was carried out by Caspase-Glo 3 Assay according to the manufacturer's instruction (Promega, USA). CGCs were exposed to various concentrations of AgNPs (0-2.5 μg/mL) for 24 h, and the activated caspase product was analyzed using a luminometer (Thermo, USA).

### 5.5. Evaluation of Oxidative Stress in AgNPs exposed CGCs

*Assessment of Intracellular ROS Accumulation and Total Glutathione (Reduced) Content*: Formation of intracellular ROS was measured spectrophotometrically by using the fluorescent probe DCFH-DA as previously described.[76] Briefly, CGCs were loaded with DCFH-DA (100 μM, Sigma-Aldrich, USA) for 30 min at 37 °C with 5% $CO_2$, then the cells were treated for 4 h with AgNPs (0-2.5 μg/mL). $H_2O_2$ (1 mM) was used as the positive control; the fluorescence was measured using a microplate spectrofluorometer (Thermo, Electron, USA) with excitation and emission wavelengths at 485 nm and 530 nm, respectively.

After CGCs were exposed to AgNPs for 4 h, the reduced glutathione (GSH) levels were measured by Glutathione Assay Kit (Promega, USA) following the operation procedures in the specifications. The fluorescence was evaluated by luminometry.

*Assessment of Intracellular Calcium Ion Concentration*: CGCs grown on the plates were loaded with Fura-2/AM (5 μM, Sigma-Aldrich, USA) for 30 min in PBS without calcium and magnesium ions at 37 °C with 5% $CO_2$ before exposure. The increase of intracellular $Ca^{2+}$ was expressed as the fluorescence intensity ratio measured at 340 nm and 380 nm excitation wavelength (F340/F380), as it is proportional to calcium ion concentrations. One F340/F380 ratiometric measurement of emission at 510 nm was obtained every 50 s. The experiment was carried out in the dark.

### 5.6. In vivo Evaluation of AgNP-Induced Neurotoxicity

*Animal Models and Intranasal Instillation*: Neonatal SD rats were purchased from Peking University Health Science Center at 0 days of age (initially weighting 4-5 g). All of the animal experiments adhered to the principles of care and use of laboratory animals and were approved by the Institutional Animal Care and Use Committee of Peking University. Neonatal SD rats used in this study were housed in clear plastic cages with their mother rats. The animals were maintained in a temperature-, humidity-, and light-controlled environment with a 12 h light/dark cycle. AgNPs at different concentrations were given to SD rats via intranasal instillation. All the groups were administered with AgNPs nasal drops or the vehicle control once every 24 h for 21 consecutive days.

*Measurement of Silver in the Cerebellum*: After AgNPs exposure for 21 days, the cerebellums of rats were

  

immediately collected and the total silver content in cerebellum tissues was measured by ICP-MS (Agilent 7500ce, USA) after microwave assisted digestion.[77]

*Histological Observation for Brain Slices*: Hematoxylin-eosin (H&E) staining was performed on paraffin sections of cerebellum that were dissected from rats on day 21. Briefly, after AgNPs exposure for 21 days, rats were deeply anaesthetized by intraperitoneal injection of appropriate amounts of ketamine, then perfusion fixation was performed as described previously.[78] The 5-μm-thick sections of the cerebellums were cut. After H&E staining, pathological changes were observed.[79]

*Caspase-3 Expression in Cerebellum by Western Blot*: The cerebellums of rats were removed and dissected within 5 min after sacrificed, followed by placed in cold buffer containing complete protease inhibitor (Roche, EDTA-free Protease Inhibitor Cocktail Tablets, USA) and homogenized within 2 h after collection. Cerebellum tissues from individual animals were homogenized in buffer (0.5 mL) containing complete protease inhibitor (per 100 mg tissue).[80] Equal amounts of total proteins were loaded and then the western blotting was performed as described above.

### 5.7. Statistical Analysis

All the experiments were repeated at least three times. Results are expressed as the mean ± standard deviation (SD). All results were analyzed by Student's t-test or ANOVA test. A P-value less than 0.05 was considered as statistically significant, while a P-value less than 0.005 was considered as highly significant.

## Acknowledgements

*This work was supported by the National Natural Science Foundation of China (20977100, 21107130, 21075130), 863 Project (2009AA06Z407) and the National Basic Research Program of China (2009CB421605, 2011CB936001). We gratefully acknowledge Yang Zhang from Beijing Friendship Hospital for assistance in animal experiments.*

[1] R. F. Service, *Science* **2003**, *300*, 243.
[2] F. Zhao, Y. Zhao, Y. Liu, X. Chang, C. Chen, Y. Zhao, *Small* **2011**, *7*, 1322–1337.
[3] M. Ahamed, M. S. AlSalhi, M. K. J. Siddiqui, *Clinica. Chimica. Acta.* **2010**, *411*, 1841–1848.
[4] D. Cheng, J. Yang, Y. Zhao, *Chin. Med. Equip. J.* **2004**, *4*, 26–32.
[5] H. Y. Lee, H. K. Park, Y. M. Lee, K. Kim, S. B. Park, *Chem. Commun.* **2007**, *28*, 2959–2961.
[6] P. Jain, T. Pradeep, *Biotechnol. Bioeng.* **2005**, *90*, 59–63.
[7] Y. Y. Zhang, J. Sun, *Chin. J. Med. Instrum.* **2007**, *31*, 35–38.
[8] W. P. W. Susan, J. G. M. P. Willie, A. H. Carla, I. H. Werner, G. O. Agnes, H. W. H. Evelyn, R. Boris, B. Julia, G. Iise, V. D. M. Dik, D. Susan, H. D. J. Wim, V. Z. Maaike, J. A. M. S. Adrienne, E. G. Robert, *Nanotoxicology* **2009**, *3*, 109–138.
[9] Y. S. Kim, J. S. Kim, H. S. Cho, D. S. Rha, J. M. Kim, J. D. Park, B. S. Choi, R. Lim, H. K. Chang, Y. H. Chung, I. H. Kwon, J. Jeong, B. S. Han, I. J. Yu, *Inhal. Toxicol.* **2008**, *20*, 575–583.
[10] S. Arora, J. Jain, J. M. Rajwade, K. M. Paknikar, *Toxicol. Lett.* **2008**, *179*, 93–100.
[11] S. Arora, J. Jain, J. M. Rajwade, K. M. Paknikar, *Toxicol. Appl. Pharmacol.* **2009**, *236*, 310–318.
[12] K. Soto, K. M. Garza, L. E. Murr, *Acta Biomater.* **2007**, *3*, 351–358.
[13] L. Braydich-Stolle, S. Hussain, J. J. Schlager, M. C. Hofmann, *Toxicol. Sci.* **2005**, *88*, 412–419.
[14] C. M. Powers, A. R. Badireddy, I. T. Ryde, F. J. Seidler, T. A. Slotkin, *Environ. Health. Persp.* **2011**, *119*, 37–44.
[15] J. Tang, L. Xiong, S. Wang, J. Wang, L. Liu, J. Li, F. Yuan, T. Xi, *J. Nanosci. Nanotechnol.* **2009**, *9*, 4924–4932.
[16] W. Y. Kim, J. Kim, J. D. Park, H. Y. Ryu, I. J. Yu, *J. Toxicol. Env. Heal. A* **2009**, *72*, 1279–1284.
[17] W. G. Kreyling, M. Semmler-Behnke, W. Möller, *J. Nanopart. Res.* **2006**, *8*, 543–562.
[18] P. H. Hoet, I. Bruske-Hohlfeld, O. V. Salata, *J. Nanobiotechnol.* **2004**, *2*, 12.
[19] J. Tang, L. Xiong, G. Zhou, S. Wang, J. Wang, L. Liu, J. Li, F. Yuan, S. Lu, Z. Wan, L. Chou, T. Xi, *J. Nanosci. Nanotechnol.* **2010**, *10*, 6313–6317.
[20] W. J. Trickler, S. M. Lantz, R. C. Murdock, A. M. Schrand, B. L. Robinson, G. D. Newport, J. J. Schlager, S. J. Oldenburg, M. G. Paule, W. J. Slikker, S. M. Hussain, S. F. Ali, *Toxicol. Sci.* **2010**, *118*, 160–170.
[21] G. Oberdörster, Z. Sharp, V. Atudorei, A. Elder, R. Gelein, W. Kreyling, C. Cox, *Inhal. Toxicol.* **2004**, *16*, 437–445.
[22] L. Ye, G. Wei, G. Ren, Z. Yang, *Toxicol. Lett.* **2012**, *209*, 227- 231.
[23] H. Zhang, T. Xia, H. Meng, M. Xue, S. George, Z. Ji, X. Wang, R. Liu, M. Wang, B. France, R. Rallo, R. Damoiseaux, Y. Cohen, K. A. Bradley, J. I. Zink, A. E. Nel, *ACS Nano* **2011**, *5*, 2756–2769.
[24] J. Zurlo, L. M. Arterburn, *In Vitro Cell. Dev. Biol.* **1996**, *32*, 211–220.
[25] N. Miura, Y. Shinohara, *Biochem. Bioph. Res. Co.* **2009**, *390*, 733–737.
[26] W. Liu, Y. Wu, C. Wang, H. C. Li, T. Wang, C. Y. Liao, L. Cui, Q. F. Zhou, B. Yan, G. B. Jiang, *Nanotoxicology* **2010**, *4*, 319–330.
[27] M. Ahamed, R. Posgai, T. J. Gorey, M. Nielsen, S. M. Hussain, I. J. Rowe, *Toxicol. Appl. Pharmacol.* **2010**, *242*, 263–269.
[28] T. Reistad, E. Mariussen, A. Ring, F. Fonnum, *Toxicol. Sci.* **2007**, *96*, 268–278.
[29] A. Pompella, A. Visvikis, A. Paolicchi, V. D. Tata, A. F. Casini, *Biochem. Pharmacol.* **2003**, *66*, 1499–503.
[30] M. L. Circu, T. Y. Aw, *Free Radical Res.* **2008**, *42*, 689–706.
[31] R. J. Whit, I. J. Reynolds, *J. Neurosci.* **1996**, *16*, 5688–5697.
[32] V. K. M. Poon, A. Burd, *Burns* **2004**, *30*, 140–7.
[33] S. M. Hussain, K. L. Hess, J. M. Gearhart, K. T. Geiss, J. J. Schlager, *Toxicol. In Vitro* **2005**, *19*, 975–983.
[34] M. Ahamed, M. Karns, M. Goodson, J. Rowe, S. M. Hussain, J. J. Schlager, Y. Hong, *Toxicol. Appl. Pharmacol.* **2008**, *233*, 404–410.
[35] H. Y. Lee, Y. J. Choi, E. J. Jung, H. Q. Yin, J. T. Kwon, J. E. Kim, H. T. Im, M. H. Cho, J. H. Kim, H. Y. Kim, *J. Nanopart. Res.* **2010**, *12*, 1567–1578.
[36] Y. H. Hsin, C. F. Chen, S. Huang, T. S. Shih, P. S. Lai, P. J. Chueh, *Toxicol. Lett.* **2008**, *179*, 130–139.
[37] A. Haase, S. Rott, A. Mantion, P. Graf, J. Plendl, A. F. Thünemann, W. P. Meier, A. Taubert, A. Luch, G. Reiser, *Toxicol. Sci.* **2012**, *126*, 457–468.
[38] S. R. D'Mello, C. Galli. T. Ciotti, P. Calissano, *Proc. Natl. Acad. Sci. USA* **1993**, *99*, 10989–10993.
[39] N. Lewinski, V. Colvin, R Drezek, *Small* **2008**, *4*, 26–49.

  

[40] S. Barillet, M. L. Jugan, M. Laye, Y. Leconte, N. Herlin-Boime, C. Reynaud, M. Carriere, *Toxicol. Lett.* **2010**, *198*, 324–330.
[41] S. M. Hussain, K. L. Hess, J. M. Gearhart, K. T. Geiss, J. J. Schlager, *Toxicol. In Vitro* **2005**, *19*, 975–983.
[42] S. Arora, J. Jain, J. M. Rajwade, K. M. Paknikar, *Toxicol. Lett.* **2008**, *179*, 93–100.
[43] Wendelin J. Stark, *Angew. Chem. Int. Ed.* **2011**, *50*, 1242–1258.
[44] T. J. Brunner, P. Wick, P. Manser, P. Spohn, R. N. Grass, L. K. Limbach, A. Bruinink, W. J. Stark, *Environ. Sci. Technol.* **2006**, *40*, 4374–4381.
[45] J. Tang, L. Xiong, S. Wang, J. Wang, L. Liu, J. Li, F. Yuan, T. Xi, *J. Nanosci. Nanotechnol.* **2009**, *9*, 4924–4932.
[46] B. Schutte, R. Nuydens, H. Geerts, F. Ramaekers, *J. Neurosci. Meth.* **1998**, *86*, 63–69.
[47] D. M. Geddes, R. S. Cargill, M. C. Laplaca, *J. Neurotraum.* **2003**, *20*, 1039–1049.
[48] S. R. Kirchhoff, S. Gupta, A. A. Knowlton, *Circulation*, **2012**, *105*, 2899–2904.
[49] R. Rosa, C. Sanfeliu, C. Sunol, A. Pomes, E. Rodriguez-farre, A. Schousboe, A. Frandsen, *Toxicol. Appl. Pharm.* **1997**, *142*, 31–39.
[50] J. Yuan, B. A. Yankner, *Nature* **2000**, *407*, 802–809.
[51] J. Yuan, M. Lipinski, A. Degterev, *Neuron* **2003**, *40*, 401–413.
[52] J. Li, J. Yuan, *Oncogene* **2008**, *27*, 6194–6206.
[53] G. M. Cohen, *Biochem. J.* **1997**, *1*, 326.
[54] M. Ahamed, M. J. Akhtar, M. A. Siddiqui, J. Ahmad, J. Musarrat, A. A. Al-Khedhairy, M. S. AlSalhi, S. A. Alrokayan, *Toxicology* **2011**, *283*, 101–108.
[55] S. J. Kang, B. M. Kim, Y. J. Lee, S. H. Hong, H. W. Chung, *Biochem Biophys Res Commun.* **2009**, *386*, 682–687.
[56] J. Zhao, L. Bowman, X. Zhang, X. Shi, B. Jiang, V. Castranova, M. Ding, *J Nanobiotechnology* **2009**, *7*, 2.
[57] P. V. AshaRani, G. L.K Mun, M. P. Hande, S. Valiyaveettil, *ACS Nano* **2009**, *3*, 279–290.
[58] M. P. Mattson, *Nat. Rev. Mol. Cell Bio.* **2000**, *1*, 120–129.
[59] L. K. Limbach, P. Wick, P. Manser, R. N. Grass, A. Bruinink, W. J. Stark, *Environ. Sci. Technol.* **2007**, *41*, 4158–4163.
[60] M. T. Lin, M. F. Beal, *Nature* **2006**, *443*, 787–795.
[61] A. S. Thakor, R. Paulmurugan, P. Kempen, C. Zavaleta, R. Sinclair, T. F. Massoud, S. S. Gambhi, *Small* **2011**, *7*, 126–136.
[62] C. C. Huang, R. S. Aronstam, D. R. Chen, Y. W. Huang, *Toxicol. In Vitro* **2010**, *24*, 45–55.
[63] B. A. Koeneman, Y. Zhang, P. Westerhoff, Y. Chen, J. C. Crittenden, D. G. Capco, *Cell Biol. Toxicol.* **2010**, *26*, 225–238.
[64] E. Jan, S. J. Byrne, M. Cuddihy, A. M. Davies, Y. Volkov, Y. K. Gun'ko, N. A. Kotov, *ACS Nano* **2008**, *2*, 928–938.
[65] P. Ariano, P. Zamburlin, A. Gilardino, R. Mortera, B. Onida, M. Tomatis, M. Ghiazza, B. Fubini, D. Lovisolo, *Small* **2011**, *7*, 766–774.
[66] D. Nijhawan, N. Hornarpour, X. Wang, *Annu. Rev. Neurosci.* **2000**, *23*, 73–87.
[67] L. S. Honig, R. N. Rosenberg, *AM. J. Med.* **2000**, *108*, 317–330.
[68] K. Loeschner, N. Hadrup, K. Qvortrup, A. Larsen, X. Gao, U. Vogel, A. Mortensen, H. R. Lam, E. H. Larsen, *Part. Fibre Toxicol.* **2011**, *8*, 18.
[69] D. P. Lankveld, A. G. Oomen, P. Krystek, A. Neigh, A. Troost-de Jong, C. W. Noorlander, J. C. Van Eijkeren, R. E. Geertsma, W. H. De Jong, *Biomaterials* **2010**, *31*, 8350–8361.
[70] L. Garza-Ocanas, D. A. Ferrer, J. Burt, L. A. Diaz-Torres, M. R. Cabrera, V. T. Rodriguez, R. L. Rangel, D. Romanovicz, M. Jose-Yacaman, *Metallomics* **2010**, *2*, 204–210.
[71] H. S. Sharma, S. F. Ali, S. M. Hussain, J. J. Schlager, A. Sharma, *J. Nanosci. Nanotechnol.* **2009**, *9*, 5055–5072.
[72] H. S. Sharma, S. F. Ali, S. M. Hussain, J.J Schlager, A. Sharma, *J. Nanosci. Nanotechno.* **2009**, *9*, 5055–5072.
[73] Q. L. Zhang, M. Q. Li, J. W. Ji, F. P. Gao, R. Bai, C. Y. Chen, Z. W. Wang, C. Zhang, Q. Niu, *Int. J. Immunopathol. Pharmacol.* **2011**, *24*, 23–29.
[74] A. Schousboe, E. Meier, J. Drejer, L. Hertz, *Preparation of Cultures of Mouse (Rat) Cerebellar Granule Cells. In A Dissection and Tissue Culture Manual for the Nervous System* (Eds: A. Shahar, J. de Vellis, A. Vernadakis, B. Haber), Alan R Liss, New York **1989**, pp. 203–206
[75] J. O'Brien, I. Wilson, T. Orton, F. Pognan, *Eur. J. Biochem.* **2000**, *267*, 5421–5426.
[76] O. Myhre, T. A. Vestad, E. Sagstuen, H. Aarnes, F. Fonnum, *Toxicol. Appl. Pharmacol.* **2000**, *167*, 222–230.
[77] S. Takenaka, E. Karg, C. Roth, H. Schulz, A. Ziesenis, U. Heinzmann, P. Schramel, J. Heyder, *Environ. Health Perspect.* **2001**, *109*, 547–551.
[78] T. Opitz, B. Scheffler, B. Steinfarz, T. Schmandt, O. Brustle, *Nat. Protoc.* **2007**, *2*, 1603–1613.
[79] A. Nehlig, E. Wittendorp-Rechenmann, C. D. Lam, *J. Cerebr. Blood F. Met.* **2004**, *24*, 1004–1014.
[80] R. L. Spencer, B. A. Kalman, C. S. Cotter, T. Deak, *Brain Res.* **2000**, *868*, 275–286.

Received: November 1, 2012
Published online: February 20, 2013

  